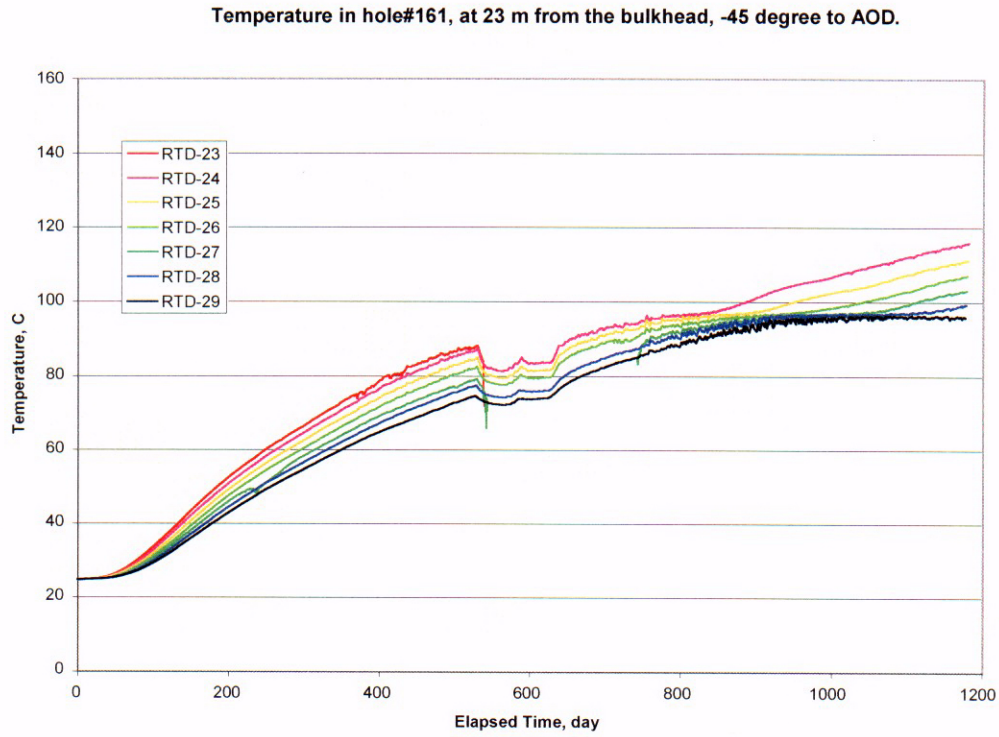

Figure 48. The almost constant temperature in borehole #161 occurs at RTD-16 to RTD-22.

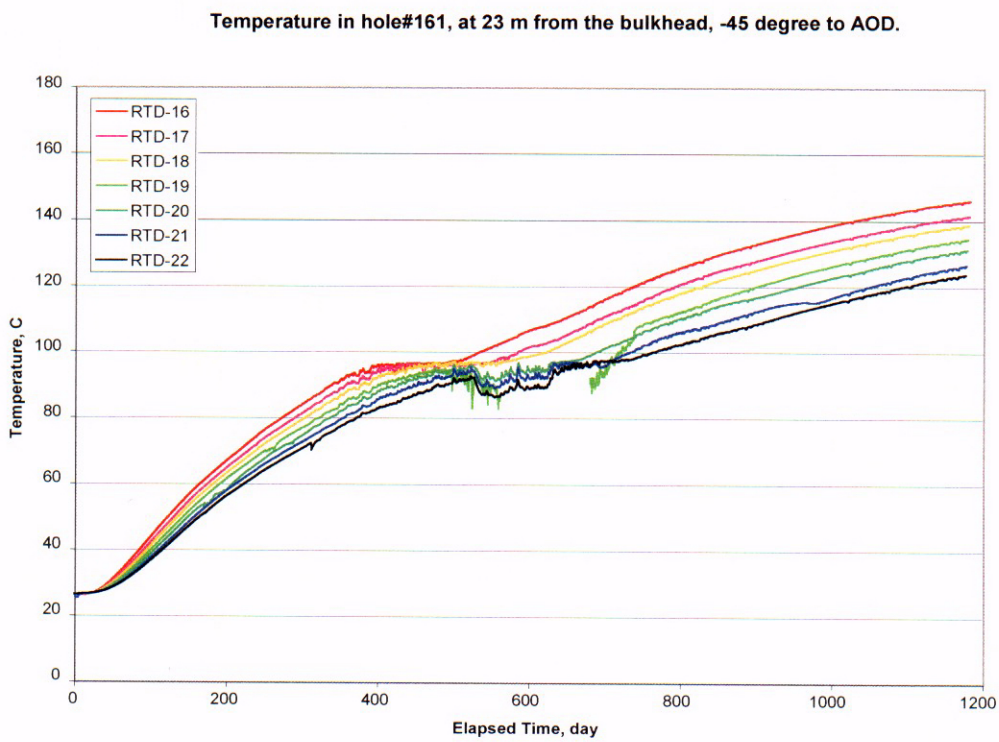

Figure 49. The almost constant temperature in borehole #161 occurs at RTD-27 to RTD-29.

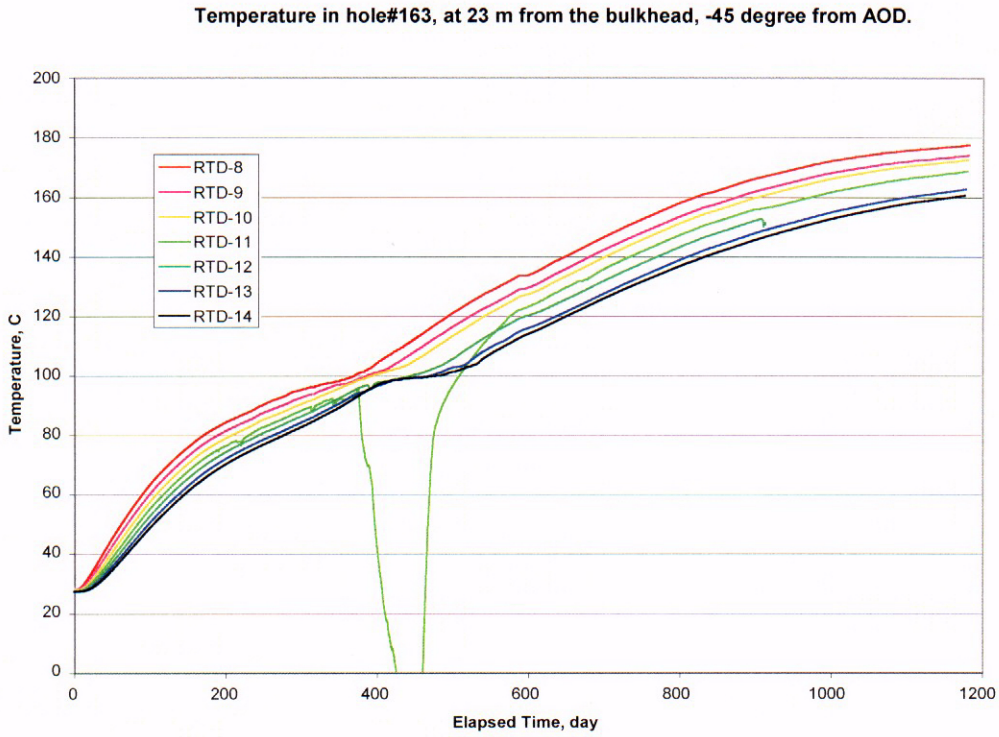

Figure 50. Rapid-evaporation process in borehole #163 develops at RTD-14. But the temperature-time curve is not very flat.

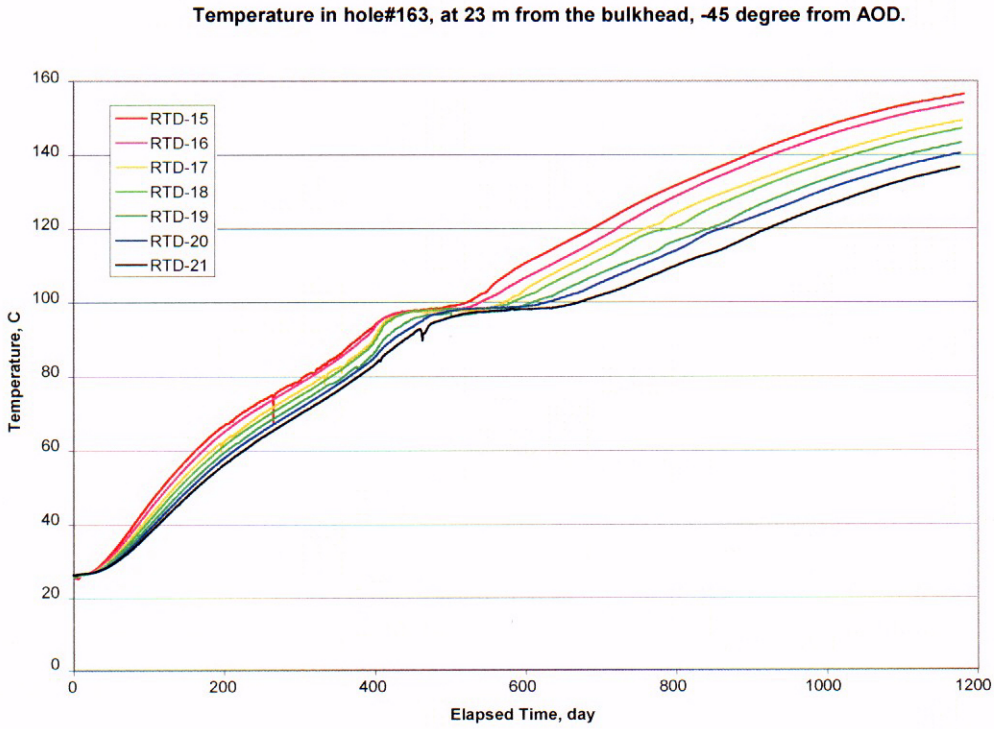

Figure 51. The temperature-time curves in borehole #163 are quite flat at RTD-16 to RTD-21.

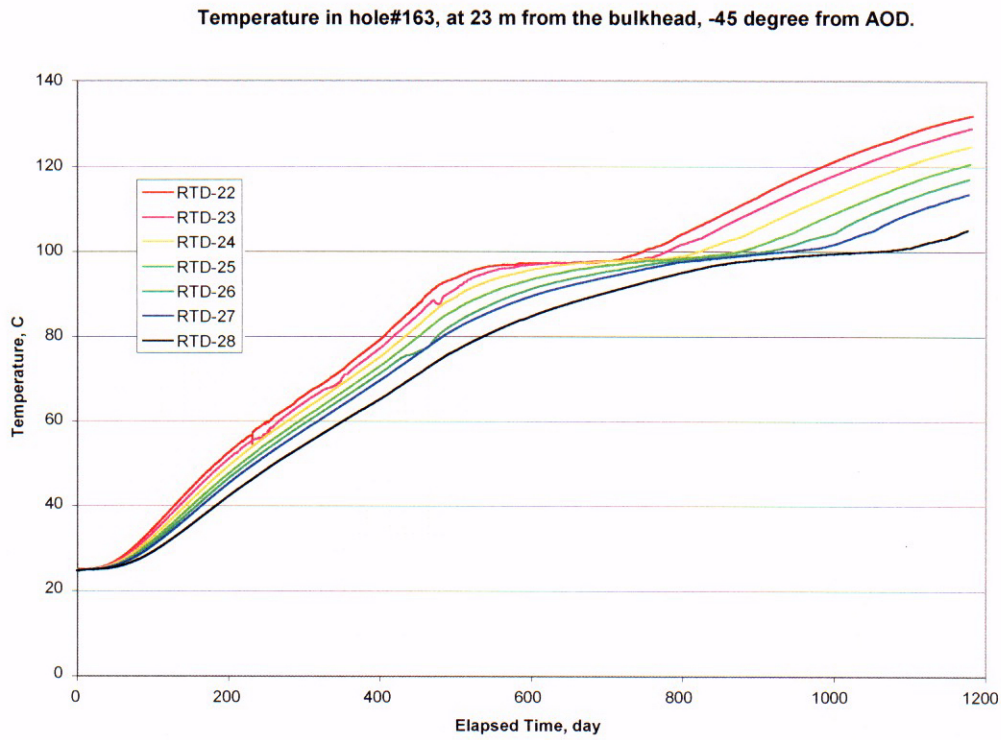

Figure 52. The temperature-time curves in borehole #163 at RTD-22 and RTD-23 have almost flat segments.

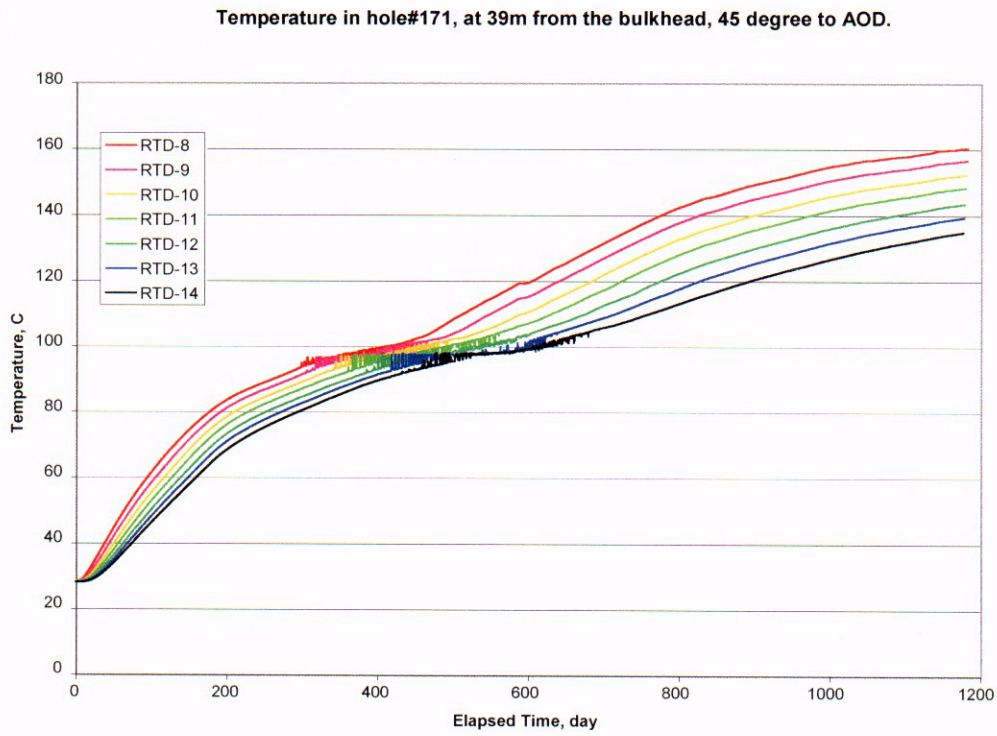

Figure 53. The temperature-time curves in borehole #171 show that the rapid evaporation process starts at RTD-13.

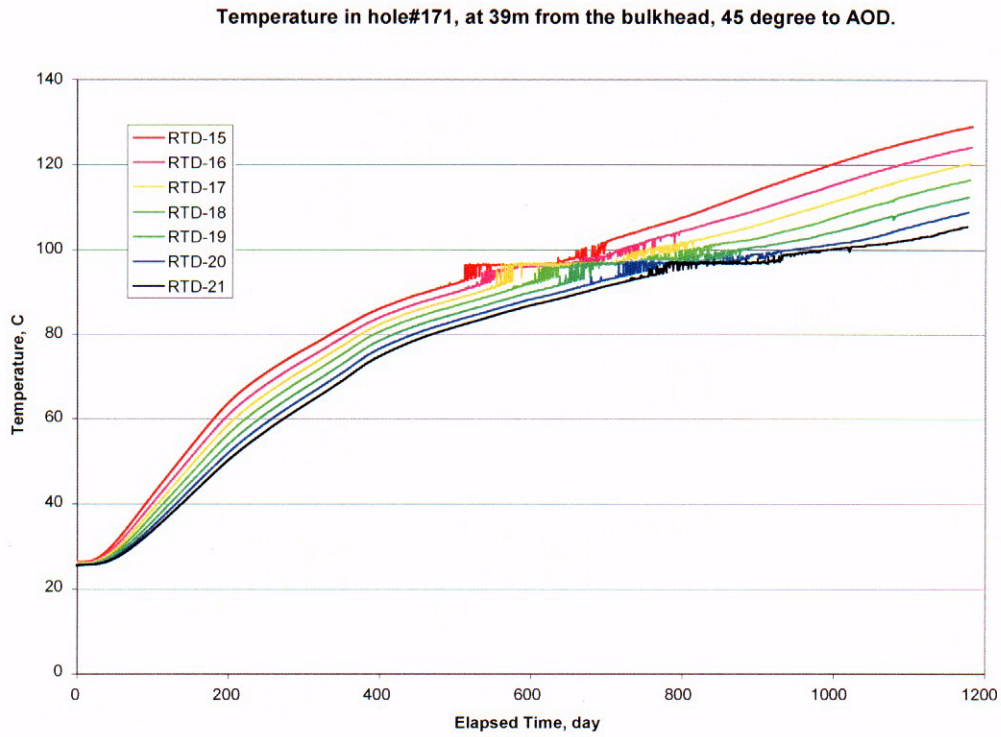

Figure 54. The temperature-time curves in borehole #171 at RTD-15 to RTD-21 have flat segments.

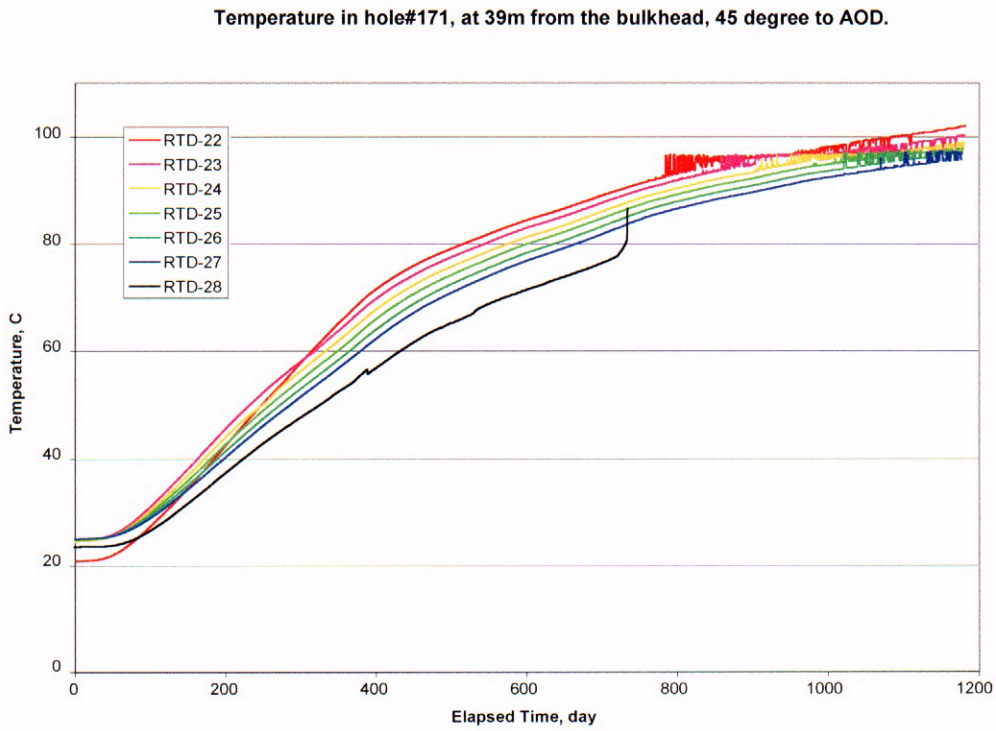

Figure 55. The temperature-time curves in borehole #171 at RTD-22 and RTD-23 show almost constant temperature periods.

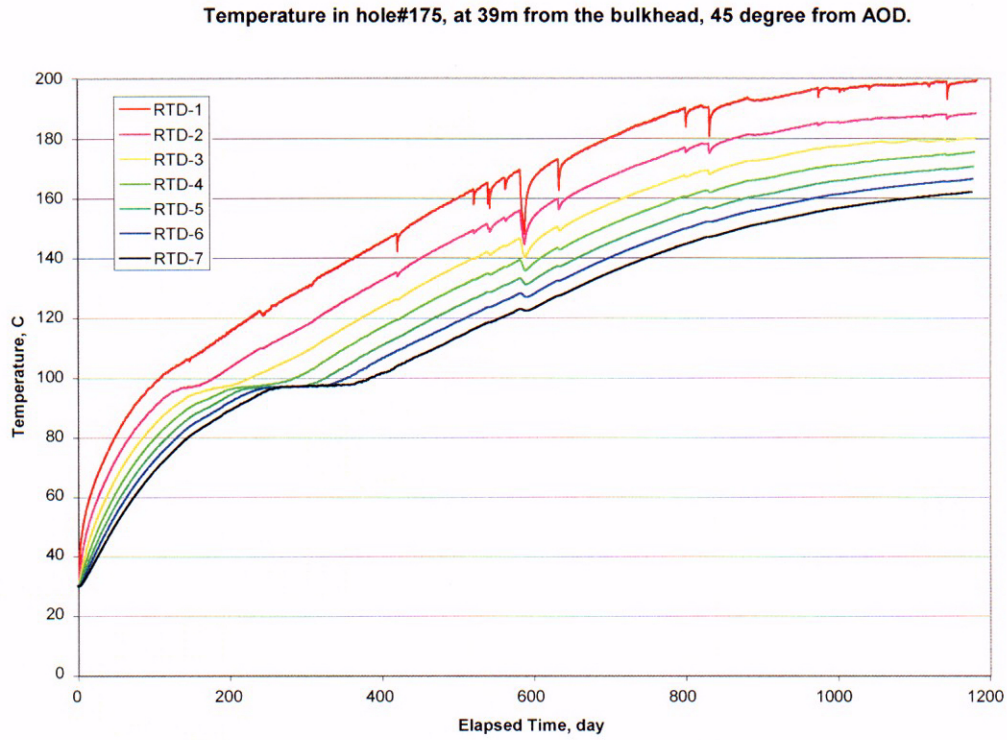

Figure 56. The temperature-time curves in borehole #175 show rapid evaporation process starts at RTD-5.

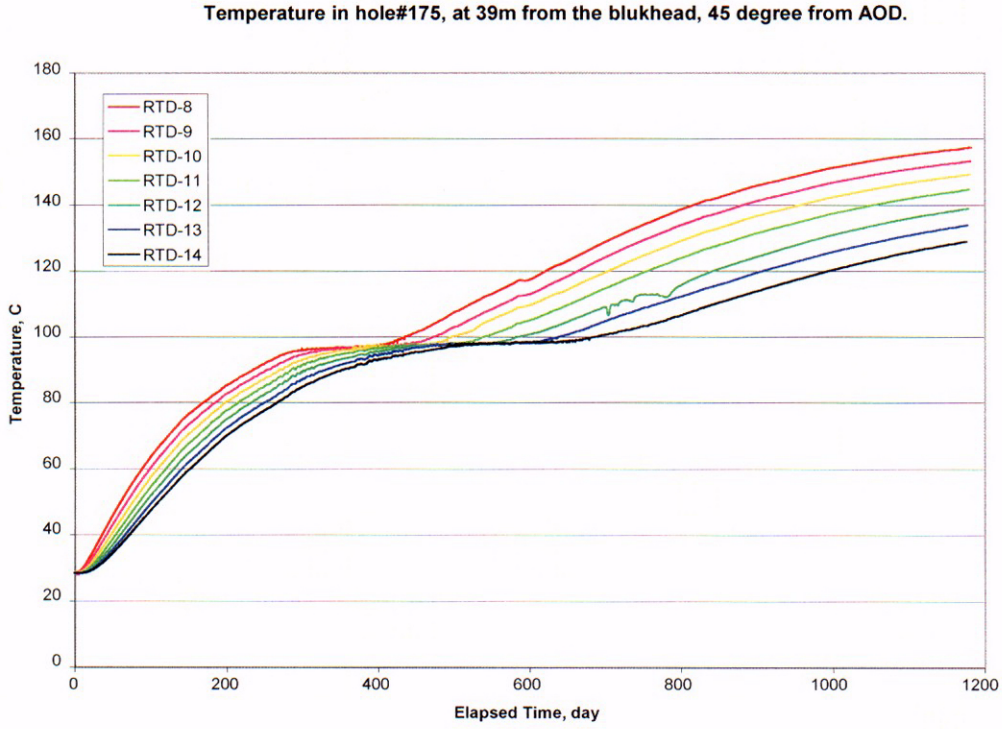

Figure 57. The temperatures in borehole #175 at RTD-8 to RTD-14 show flat regions indicating rapid evaporation.

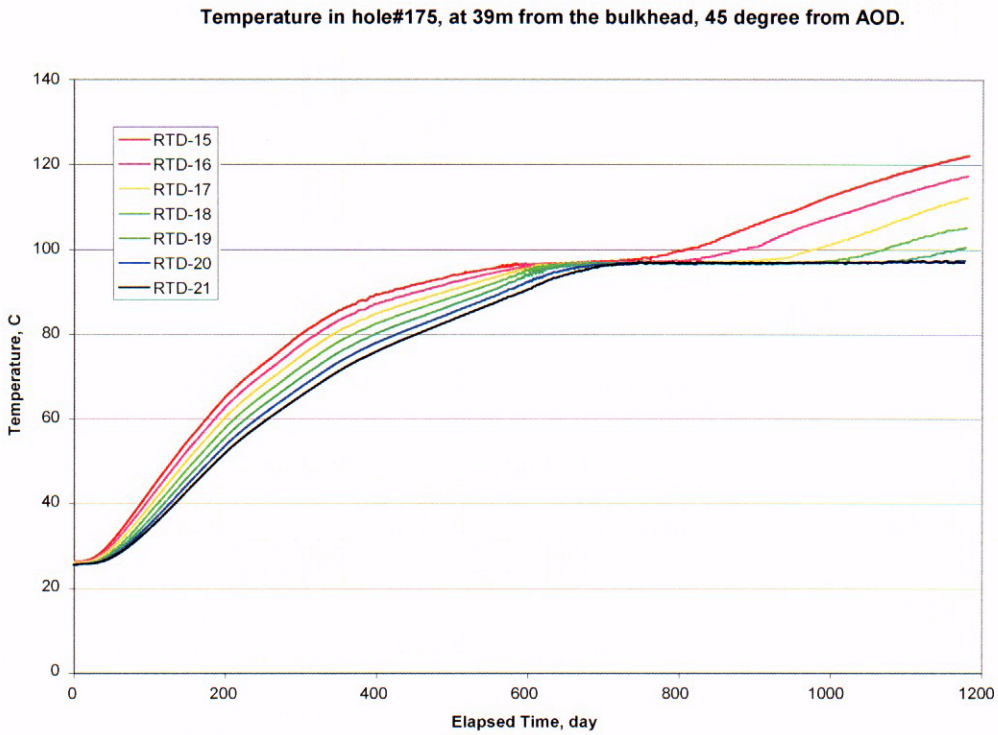

Figure 58. The temperature-time curves in borehole #175 show that the rapid evaporation process involves RTD-15 to RTD-21.

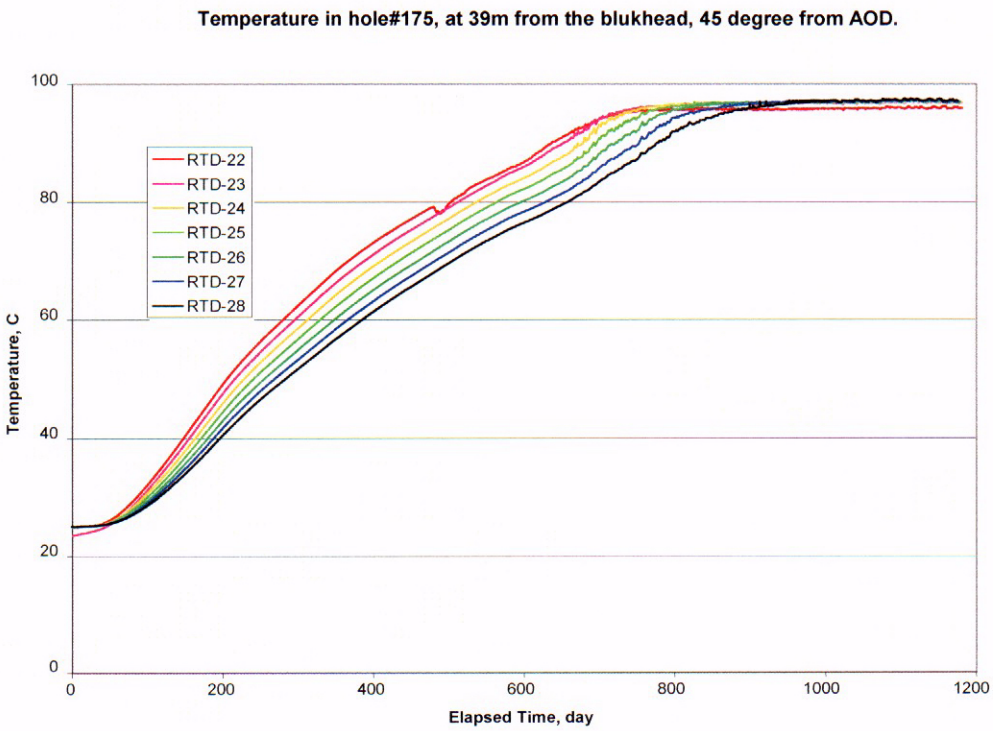

Figure 59. The temperature-time curves in borehole #175 show well-defined flat regions at RTD-22 to RTD-28.

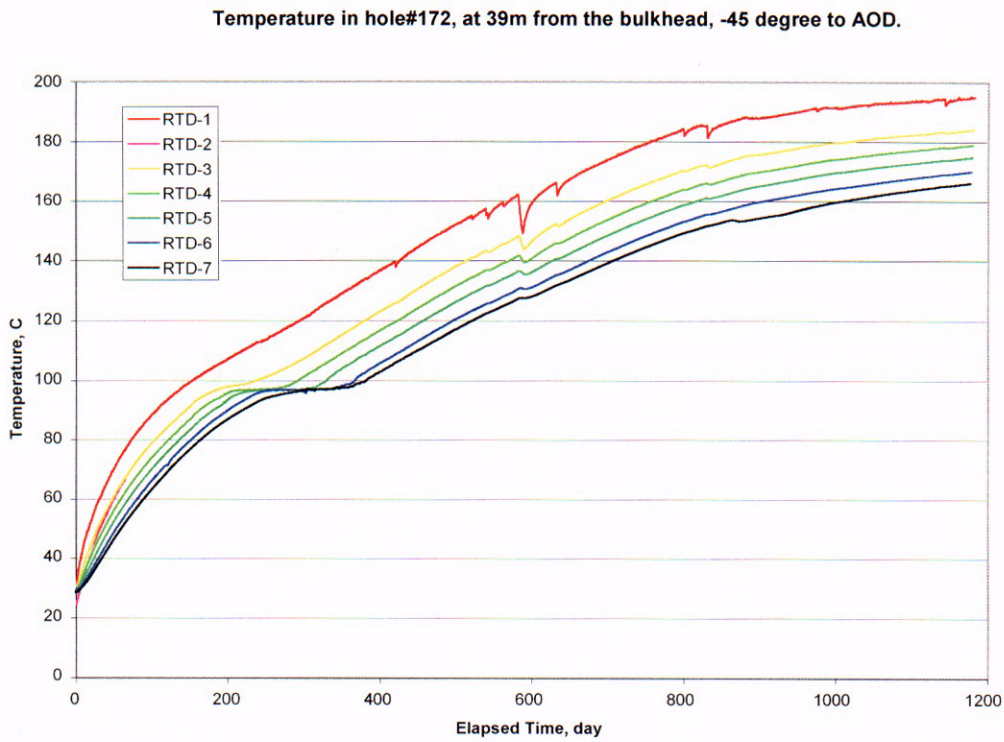

Figure 60. The temperature-time curves in borehole #172 show that the rapid evaporation process starts at RTD-4.

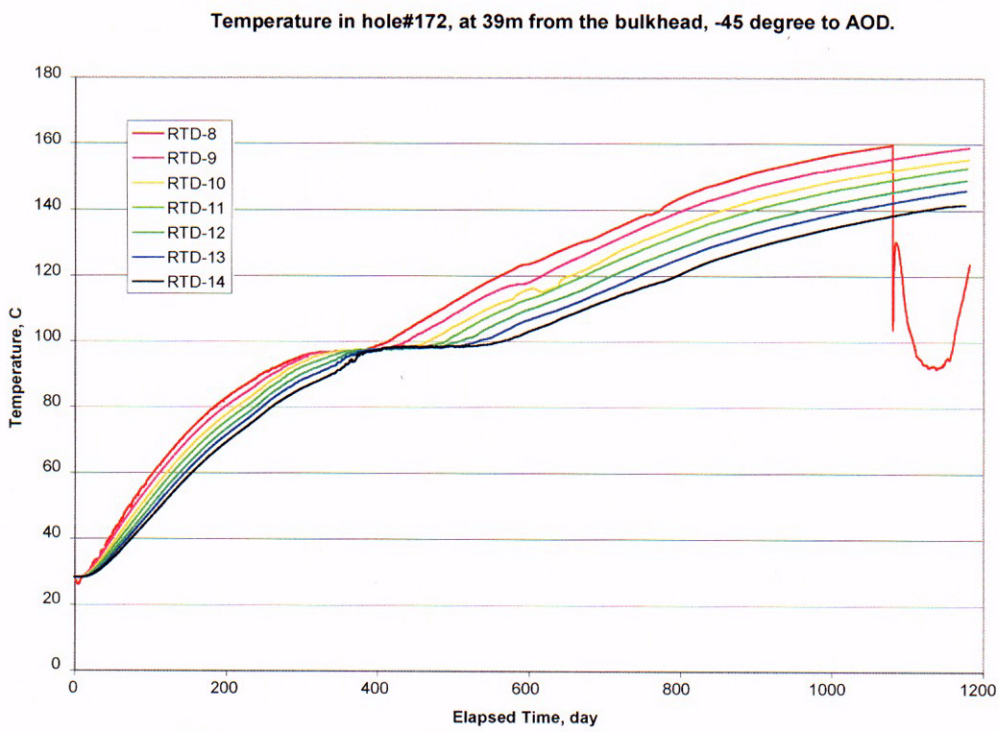

Figure 61. The temperature-time curves show that the rapid evaporation process involves all RTDs, RTD-8 to RTD-14, shown in here.

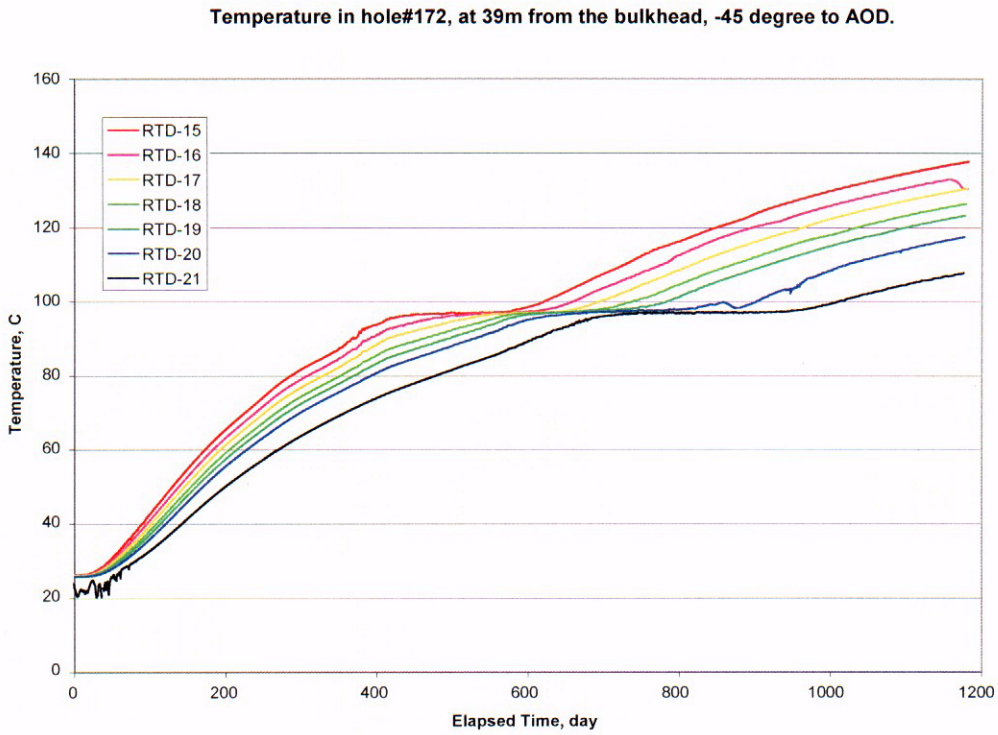

Figure 62. The temperature-time curves in borehole #172 show that RTD-15 to RTD-21 are involved in the rapid evaporation process.

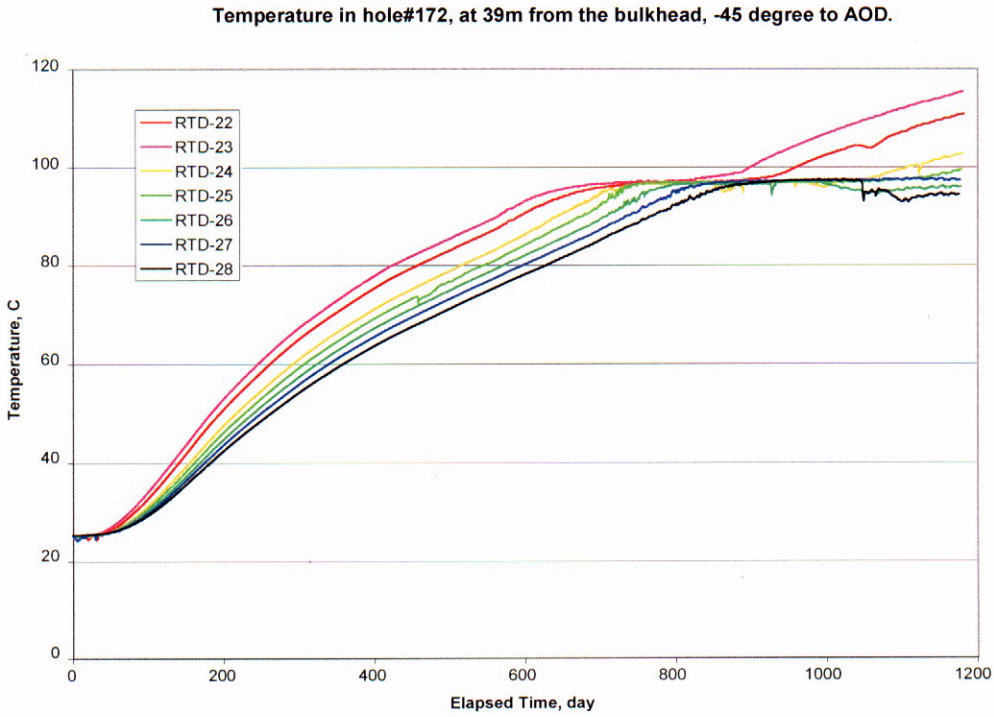

Figure 63. The temperature-time curves in borehole #172 at RTD-22 to RTD-28 show the effect of the rapid evaporation process.

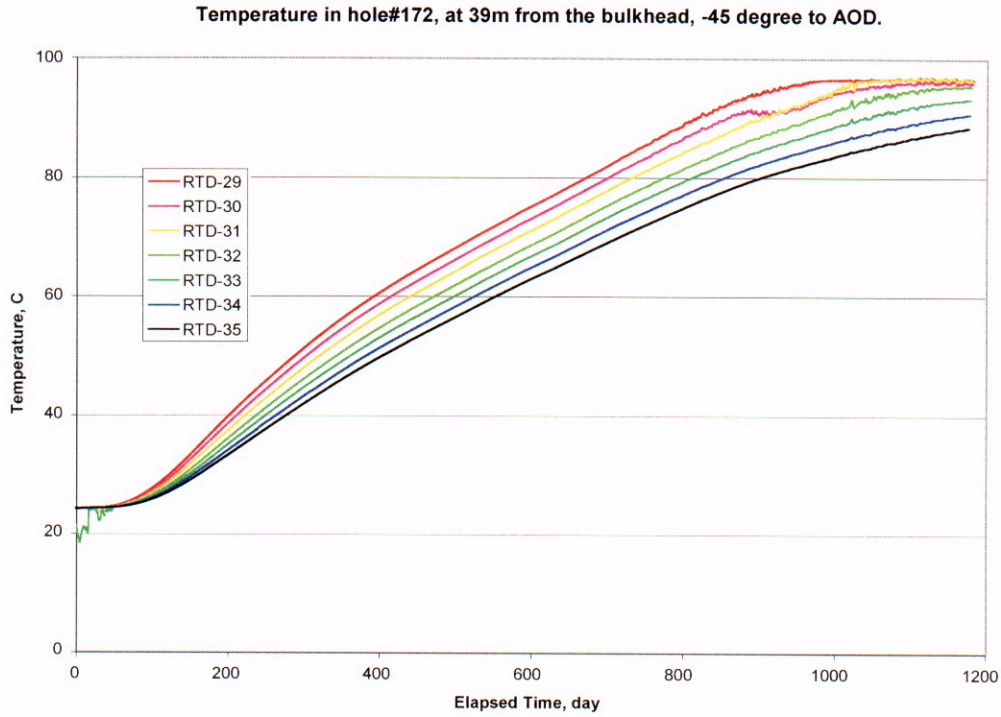

Figure 64. The temperature-time curves in borehole #172 show that at least RTD-29 to RTD-31 are involved in the rapid evaporation process.

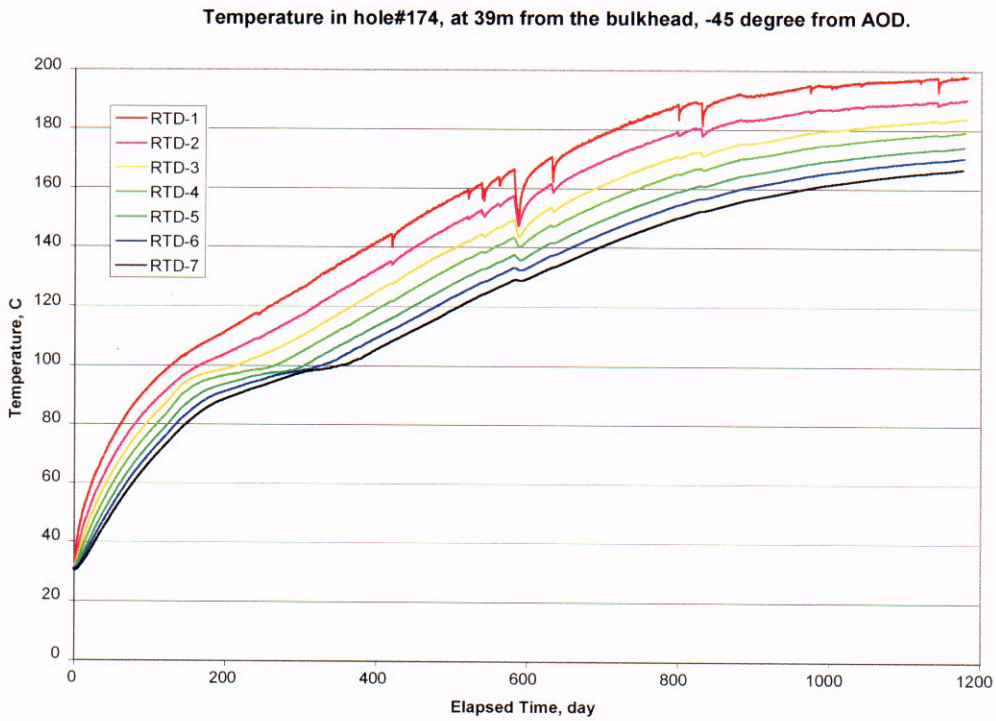

Figure 65. The temperature-time curve at RTD-7 in borehole #174 starts to show the effect of rapid evaporation.

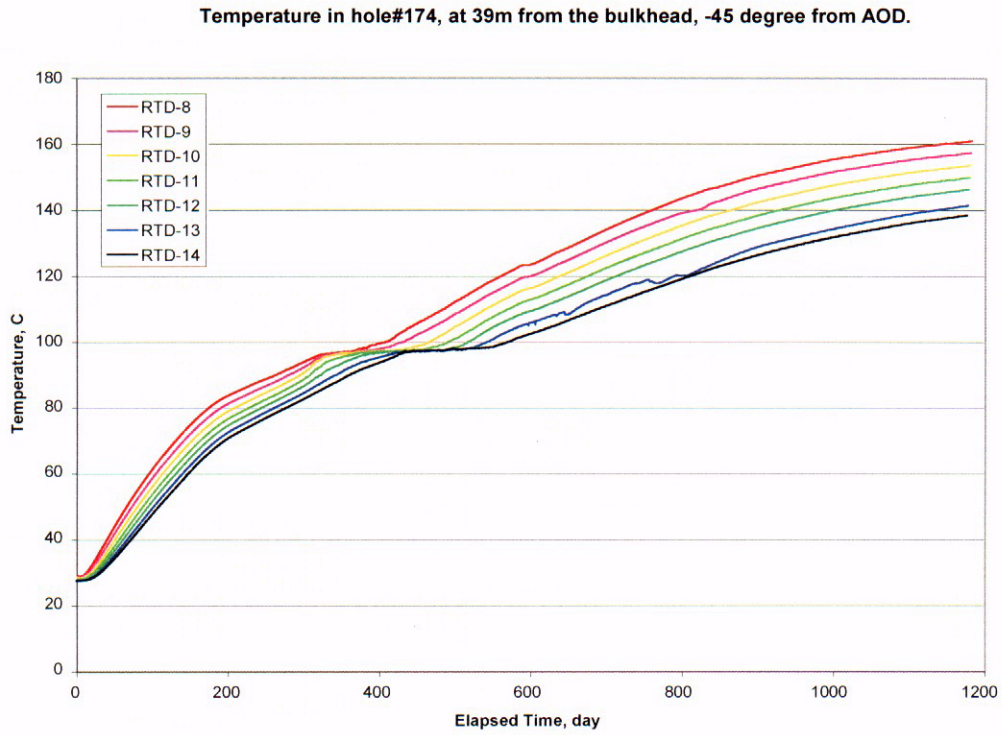

Figure 66. The temperature-time curves in borehole #174 at RTD-8 to RTD-14 show the effect of rapid evaporation.

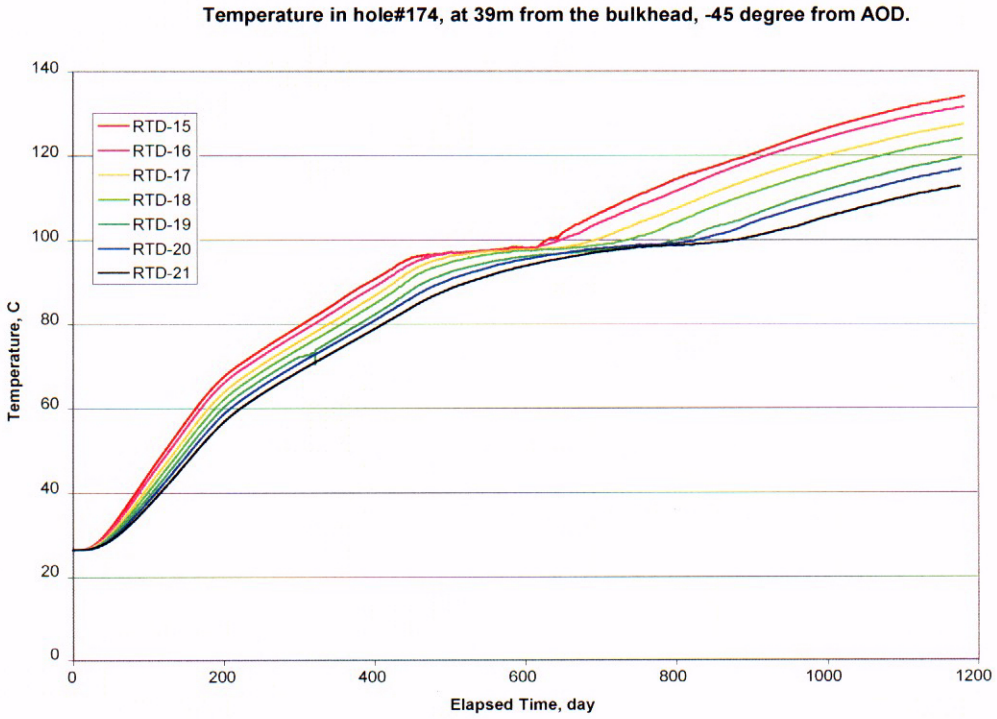

Figure 67. The temperature-time curves in borehole #174 at RTD-15 and RTD-16 show the effect of rapid evaporation.

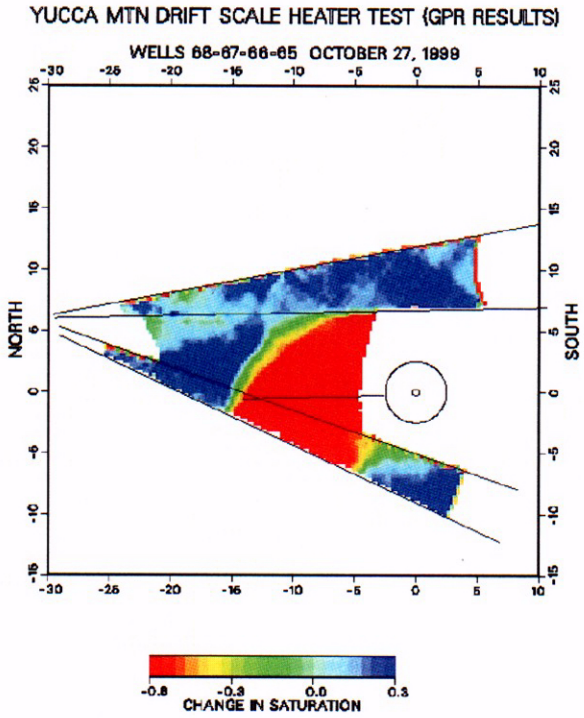

Figure 68. GPR results in boreholes #65 to #68. This figure shows the difference between the October 27, 1999 measurements and the pre-heat baseline on October 29, 1997.

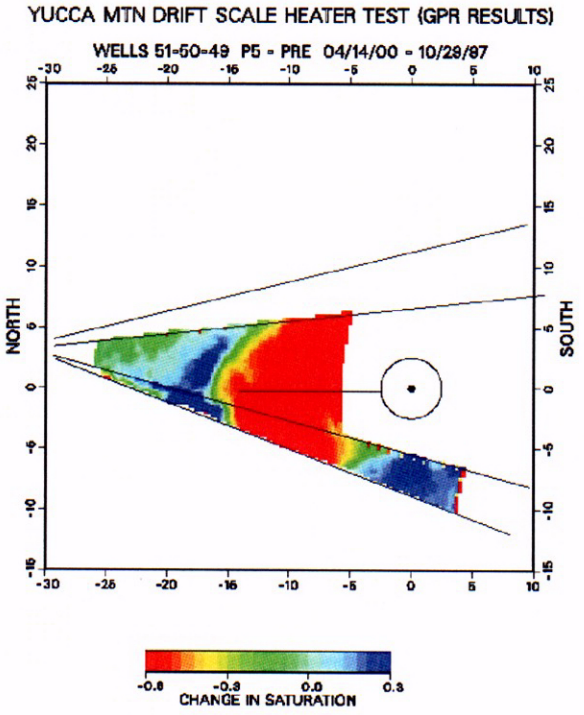

Figure 69. The GPR results in boreholes #49 to #51. This figure shows the difference between the measurements on April 14, 2000 and the pre-heat baseline on October 29, 1997.

C-40

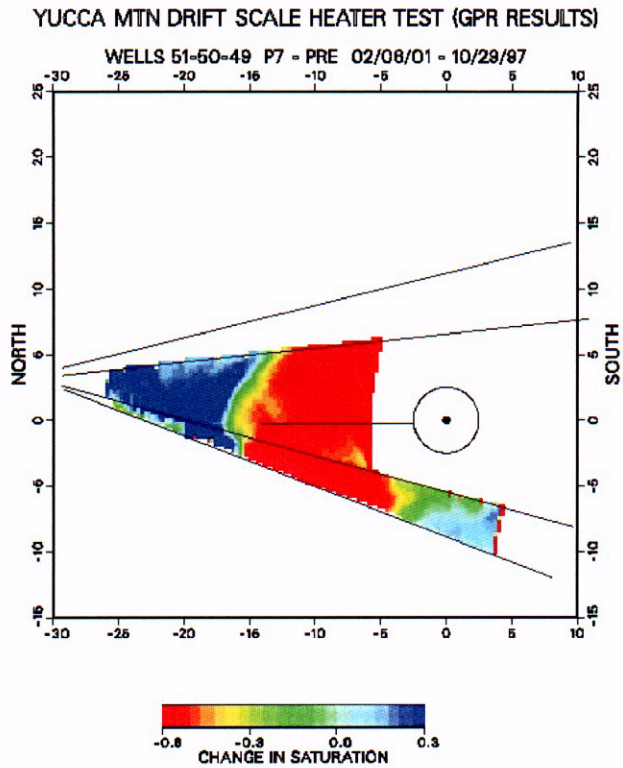

Figure 70. The GPR results in boreholes #49 to #51. This figure shows the difference between the measurements on February 6, 2001 and the pre-heat baseline on October 29, 1997.

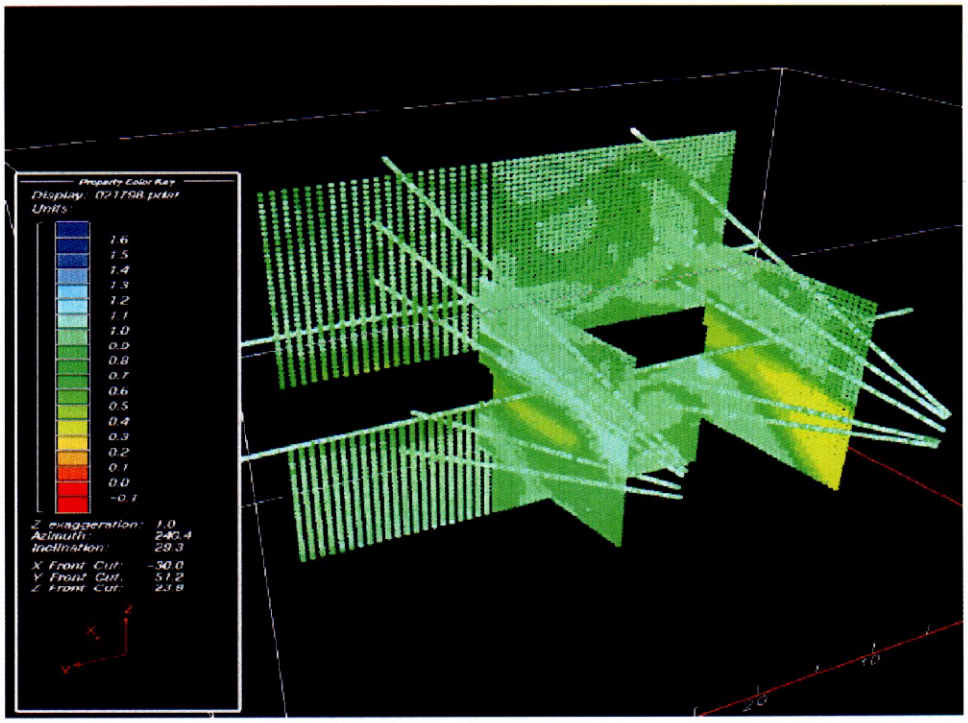

Figure 71. The ERT and neutron results in the DST. This figure shows the ratio of the water content measurements on 2/17/98 to that of the pre-heat baselines.

C-41

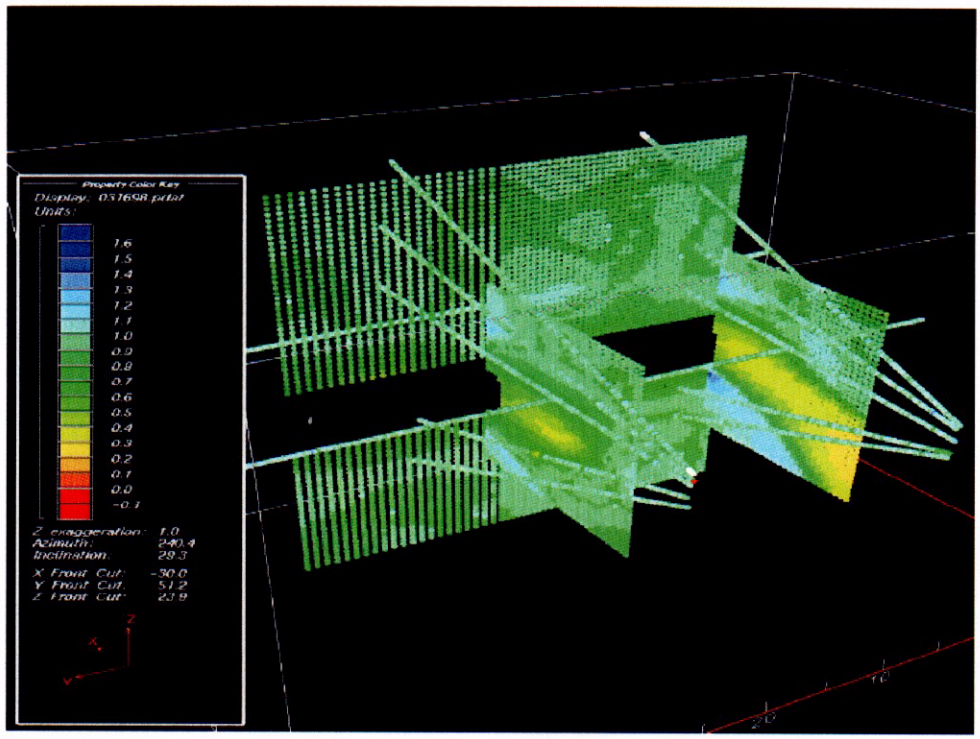

Figure 72. The ERT and neutron results in the DST. This figure shows the ratio of the water content measurements on 3/16/98 to that of the pre-heat baselines.

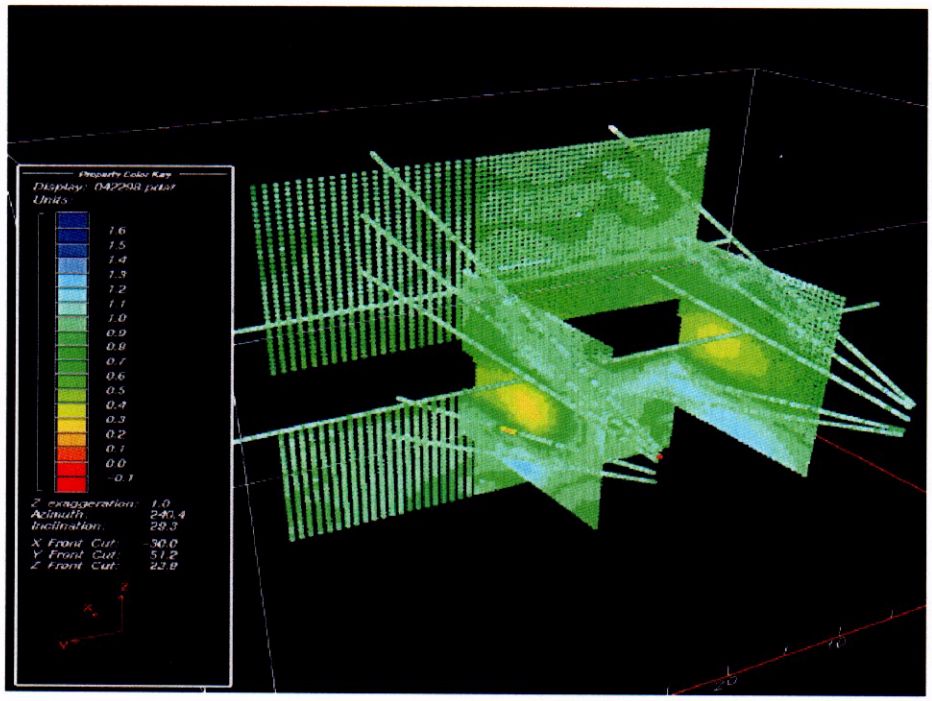

Figure 73. The ERT and neutron results in the DST. This figure shows the ratio between the water content measurements on 4/22/98 to that of the pre-heat baselines.

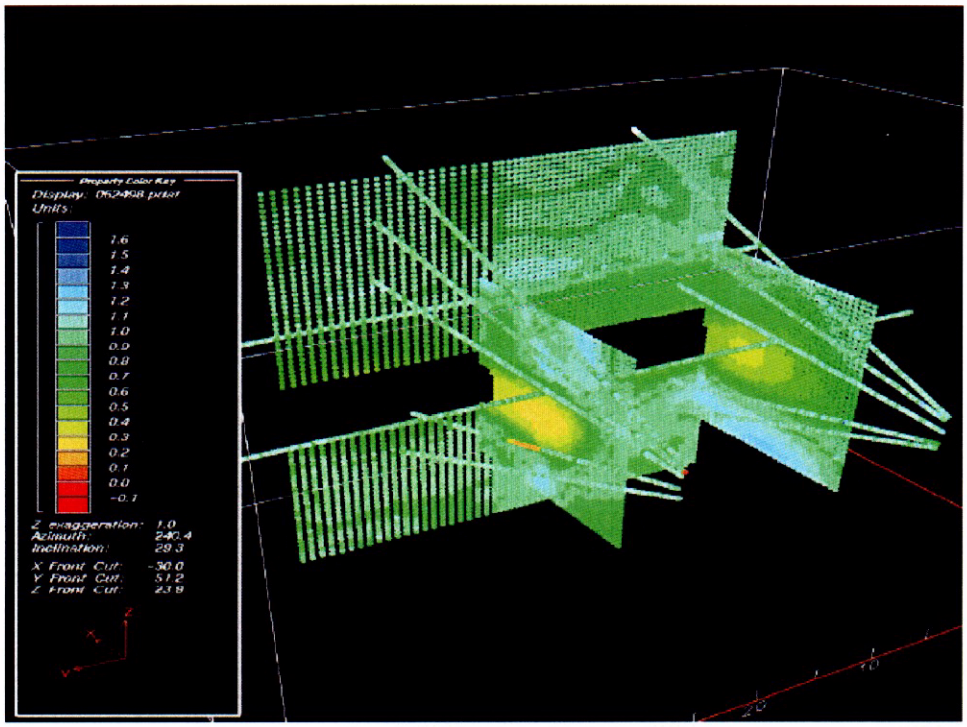

Figure 74. The ERT and neutron results in the DST. This figure shows the ratio between the water content measurements on 6/24/98 to that of the pre-heat baselines.

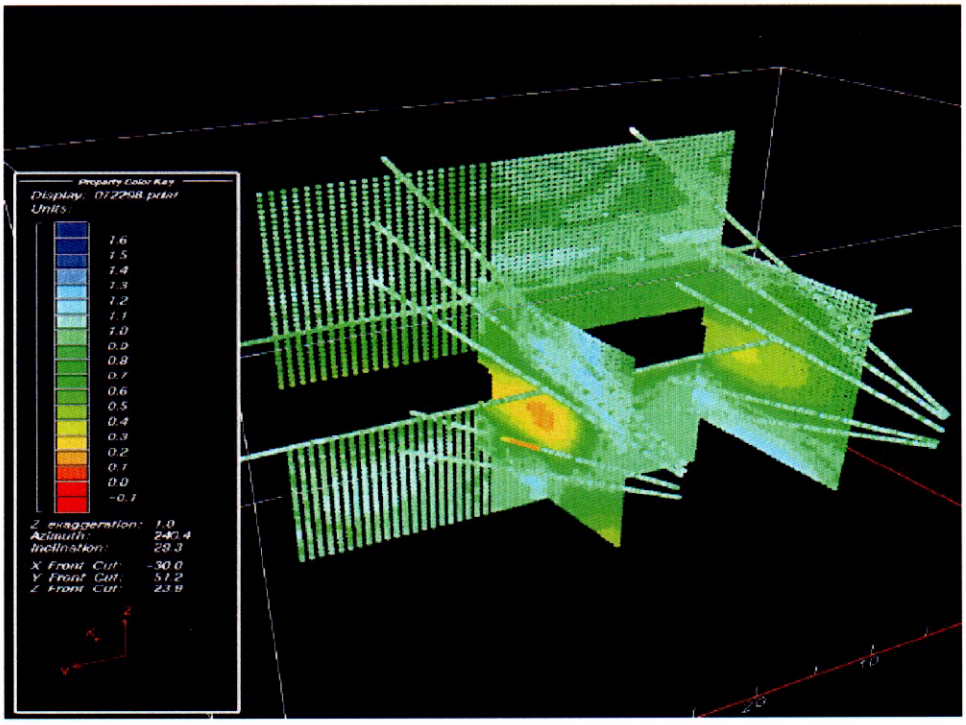

Figure 75. The ERT and neutron results in the DST. This figure shows the ratio between the water content measurements on 7/22/98 to that of the pre-heat baselines.

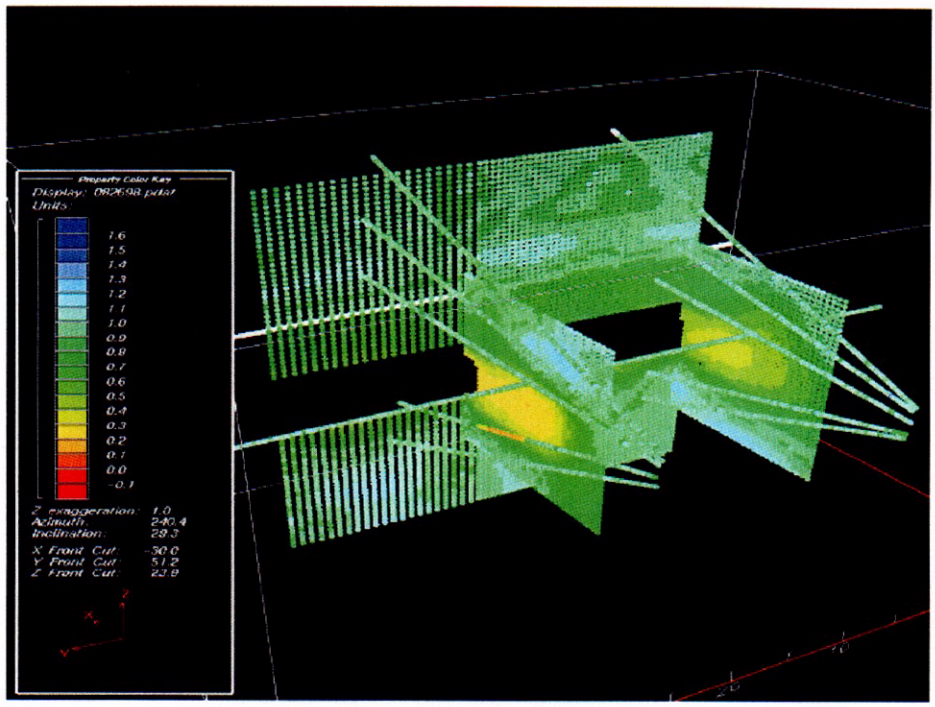

Figure 76. The ERT and neutron results in the DST. This figure shows the ratio between the water content measurements on 8/26/98 to that of the pre-heat baselines.

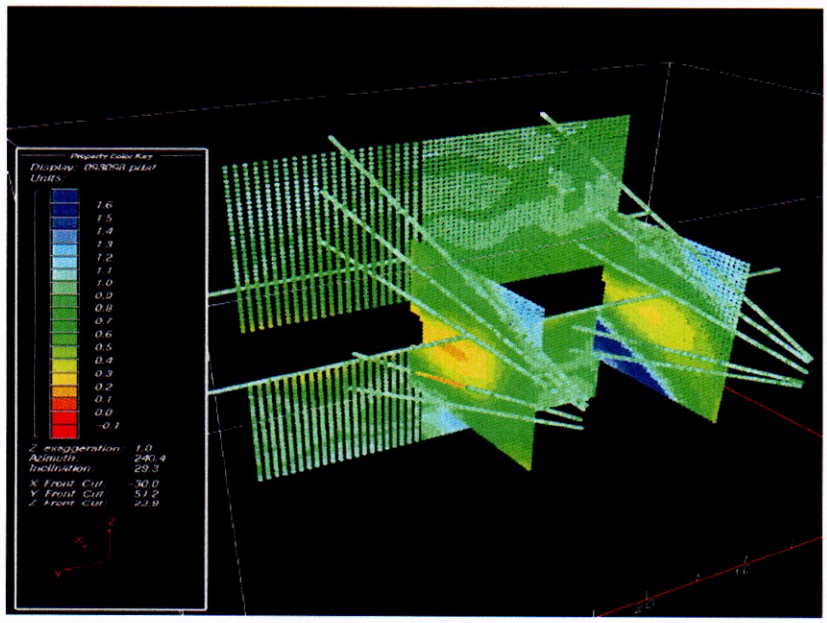

Figure 77. The ERT and neutron results in the DST. This figure shows the ratio between the water content measurements on 9/30/98 to that of the pre-heat baselines.

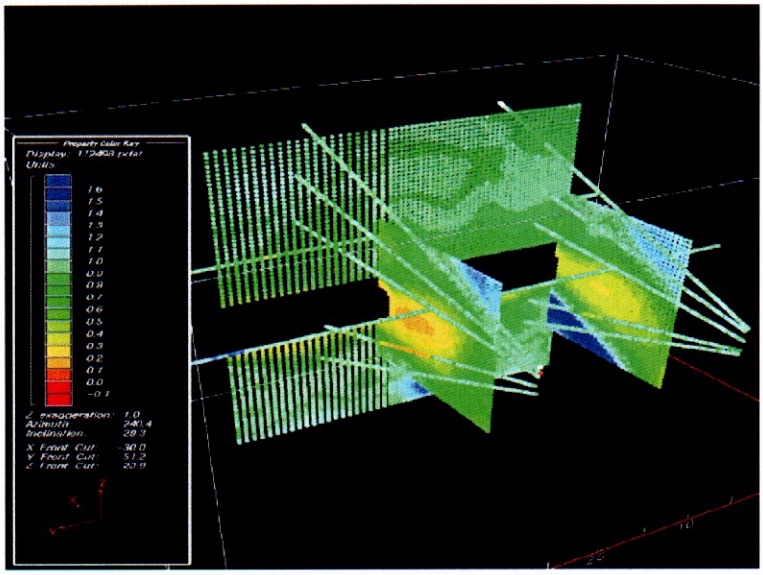

Figure 78. The ERT and neutron results in the DST. This figure shows the ratio between the water content measurements on 11/24/98 to that of the pre-heat baselines.

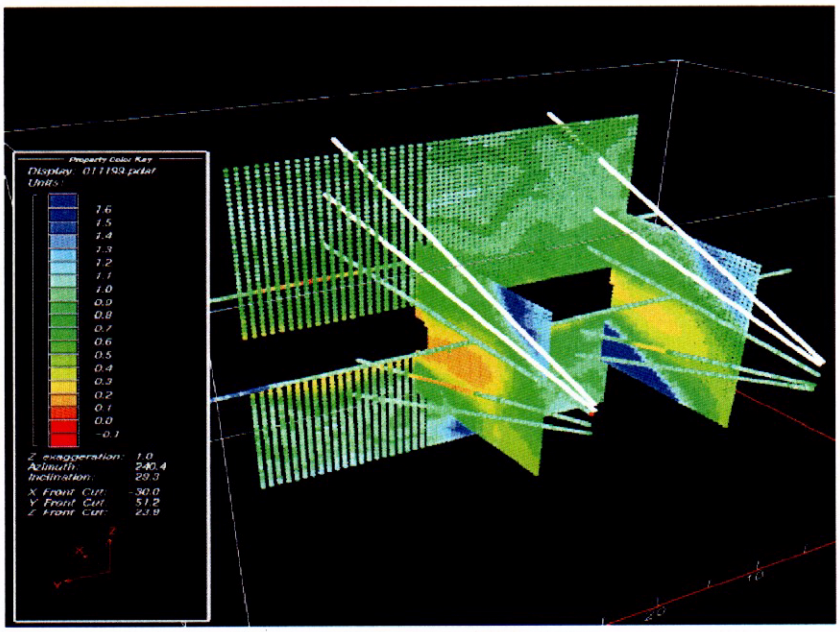

Figure 79. The ERT and neutron results in the DST. This figure shows the ratio between the water content measurements on 1/11/99 to that of the pre-heat baselines.

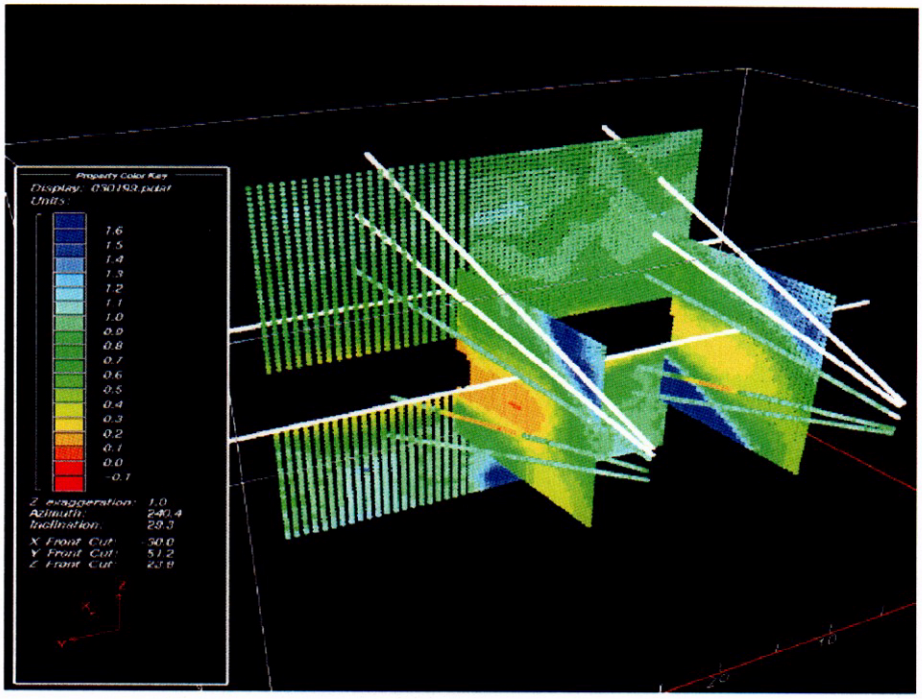

Figure 80. The ERT and neutron results in the DST. This figure shows the ratio between the water content measurements on 3/01/99 to that of the pre-heat baselines.

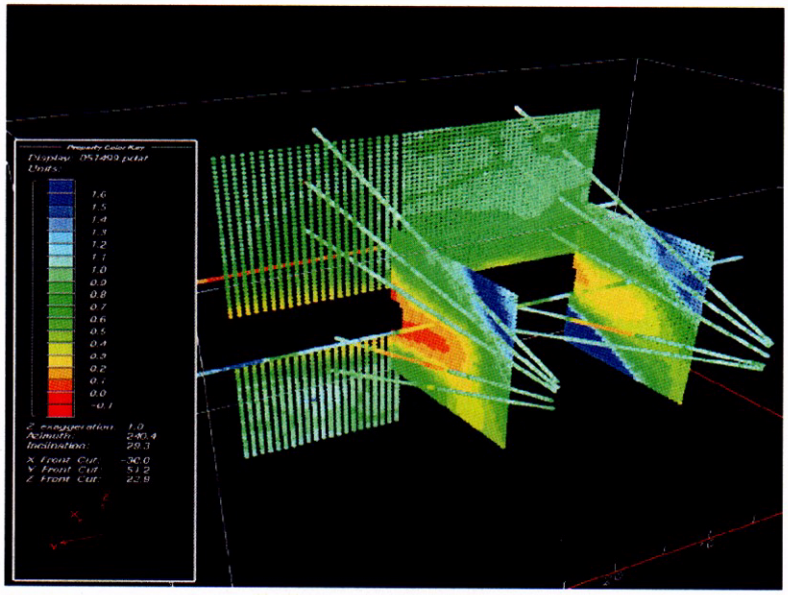

Figure 81. The ERT and neutron results in the DST. This figure shows the ratio between the water content measurements on 5/14/99 to that of the pre-heat baselines.

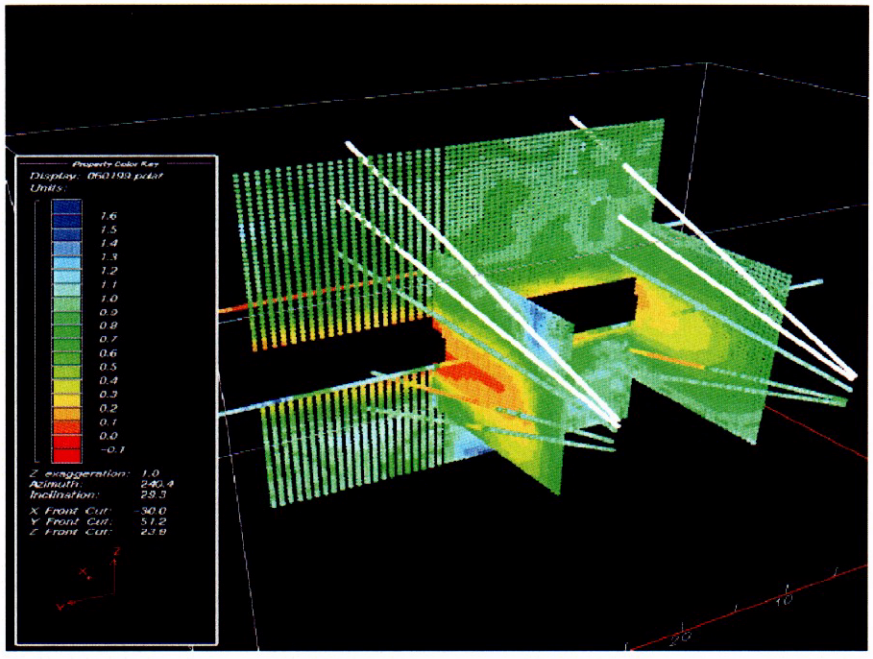

Figure 82. The ERT and neutron results in the DST. This figure shows the ratio between the water content measurements on 6/01/99 to that of the pre-heat baselines.

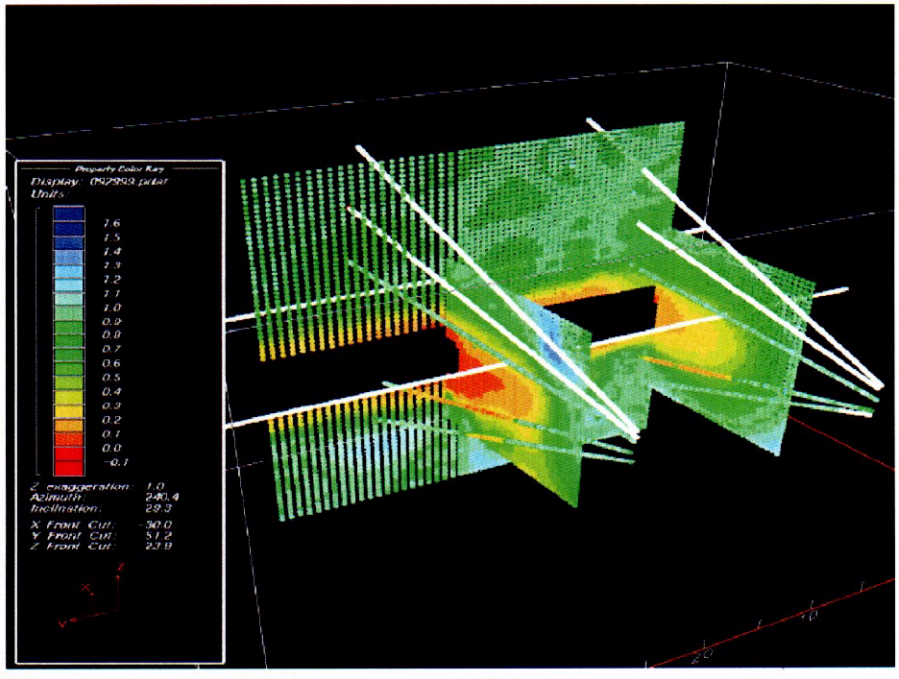

Figure 83. The ERT and neutron results in the DST. This figure shows the ratio between the water content measurements on 9/29/99 to that of the pre-heat baselines.

C-47